Ionics (2024) 30:3587–3593
https://doi.org/10.1007/s11581-024-05510-8

RESEARCH

# Impact of CTAB, a cationic surfactant, on the electrochemical performance of $NiWO_4$ for enhanced supercapacitor performance

K. Murugavel[1] · K. R. Hariprasath[2] · M. Priyadharshini[3] · P. Balaji[2] · T. Pazhanivel[2] · N. Kannadasan[4]

Received: 27 November 2023 / Revised: 26 March 2024 / Accepted: 31 March 2024 / Published online: 6 April 2024


## Abstract

In search of efficient electrode material with good redox sites, better wettability, high-rate transfer and rate capability, here we adapted a linear template method like by adding CTAB as surfactant. Transition metal tungstate is a promising electrode material for supercapacitor devices because of its exceptional electrical conductivity and electrochemical property. This work deals with the effect of surfactant on their structure, morphology and electrochemical properties of the material, elaborately. Through the physiochemical characterization, it is observed that morphology of $NiWO_4$ is stable and significantly altered by different ratio of templating agent. $NiWO_4$ with 0.03 M of CTAB as surfactant delivered a specific capacitance of about 958 F/g at a current density of 2 A/g, respectively with low-charge transfer resistance of 5.6 Ω.

**Keywords** Cationic surfactant · $NiWO_4$ · Supercapacitor

## Introduction

Energy occupies a significant role in today's world, from modern electronic gadgets to portable devices used for day to day domestic needs [1, 2]. Among various energy storage technologies like Li-ion battery and fuel cell, the supercapacitor has gained much attention due to its eminence in electrochemical performance including high durability, specific capacitance and rapid charging process than conventional capacitor and batteries [3]. Although a wide range of research was carried out to enhance the performance of supercapacitor, unfortunately still the device cannot meet the requirement of real life application due to low operating voltage, low cyclic stability and leakage of chemicals [4, 5]. Hence, now much attention is paid on improving operating voltage and cyclic stability without an appreciable loss in specific capacitance of the electrode material. To date, various materials including RuO [6], NiP [7], CoS [8, 9] and $Ni(OH)_2$ [10] were extensively investigated as an electrode material for capacitor. Recently, mixed metal oxide has drawn much interest due to the presence of multiple oxidation states which in turn provides the possibility of multiple redox reactions. With this idea, metal tungstate was considered as a potential substitute as an electrode material due to its cost effectiveness facile synthesis procedure and excellent electrical properties [11].

Generally, metal tungstates ($MWO_4$, here M stands for metals like Ni, Co, Bi, Fe, Zn, Cu) and electrode materials are highly explored due to its good environmental nature, better electrochemical response and high electric conductivity of the range of $10^{-7}$ to $10^{-3}$ $Scm^{-1}$ due to the availability of W metal. Among them, transition metal tungstates like $NiWO_4$ and $CoWO_4$ were majorly concentrated due to its better faradaic activity, high capacitance and energy density when compared to other metal tungstates. Due to its better optical, sensing and electrical properties, metal tungstates are used in various fields like photocatalysis and memory devices and humidity sensors [12–14].

Swarn Jha et al. [15] prepared $NiWO_4$ through a facile method and analysed the performance in the electrochemical behavior for a different source of nickel. The author reported a specific capacitance of about 750 F/g at 1A/g, and the

✉ N. Kannadasan
nkannadasan87@gmail.com

1 Department of Physics, Periyar University, Salem 636011, Tamil Nadu, India

2 Smart Materials Laboratory, Department of Physics, Periyar University, Salem 636011, India

3 Institut de Recherche Dupuy de Lôme, UMR CNRS 6027, 56100 Lorient, France

4 Department of Physics, Sri Sarada Mahavidhyalayam Arts and Science College for Women, Ulundurpet 606 107, Tamil Nadu, India

asymmetric-fabricated device exhibits a stability of 93% of initial capacitance over 6000 cycles. Theoretically, the reported specific capacitance was even more than the value obtained experimentally. Hence, to completely explore the efficiency of the active material optimization of different parameters to be done, a significant modification in the electrochemical performance of the prepared materials can be achieved by slightly altering the surface area and morphology of the active material.

In this work, $NiWO_4$ has been prepared successfully using surfactant (CTAB), and the variation in its physiochemical and electrochemical properties was systematically analyzed by different analytical techniques to evaluate its application for the high-performance supercapacitor application. NiWO4 with 0.03 M of CTAB as surfactant delivered a high-specific capacitance of about 958 F/g at a current density of 2 A/g, respectively with low charge transfer resistance of 5.6 Ω.

## Materials and methods

### Materials

Nickel chloride nonahydrate [$Ni(Cl)_3 9H_2O$,99%], sodium tungstate hexahydrate ($Na_2WO_4 6H_2O$,98%), cetyltrimethylpyrolidene ($C_{19}H_{42}BrN$) (CTAB), ethanol, n-methyl-2-pyrrolidene, polyvinylidene fluoride and acetylene black were purchased from Merck India Pvt Ltd. Analytical grade reagents were used in the experimental synthesis, and they were utilized without further modification.

### Preparation of $NiWO_4$

Here, 3.2 g of nickel chloride and 3.7 g sodium tungstate are dissolved in 30 ml of deionized water separately under constant stirring. After some time, sodium tungstate solution was added dropwise and stirred for 30 min. Followed by it, 0.1 g of CTAB is also added in the above solution. Later, the solution is ultrasonicated for 30 min, and then the homogeneous solution is transferred to Teflon-lined stainless-steel autoclave and maintained it for 140℃ for 12 h. The obtained products were washed with deionized water, and ethanol for three times. Then, the collected sample is dried at 70℃ for 10 h, and later the sample is calcined at 500℃ for 5 h. The resulting powder is named as NW1. Then, the process is repeated by adding different amount of CTAB (0.2 g, 0.3 g) in the above process and named as NW2 and NW3, respectively. Pure nickel tungstate ($NiWO_4$) is synthesized by following the same steps without the addition of CTAB and named as NW.

### Characterization techniques

#### Physiochemical analysis

The phase purity and crystallinity of $NiWO_4$ with different concentrations of CTAB was analyzed using the Rigaku smart lab X- ray diffractometer with Cu kα radiation ($\lambda = 1.541874$ A°). The diffracted data were collected in the range of 10°–80°. The functional group was analyzed through FTIR analysis using a Perkin Elmer RXII spectrometer. The surface morphology and elemental analysis were carried out using Carl Zeiss Sigma, Germany (scanning electron microscope).

#### Electrochemical analysis

For electrode fabrication, the as-synthesized $NiWO_4$, carbon black and PVDF (polyvinyldifluoride) were mixed with the ratio of 75:15:10. Then, the specific amount of NMP (N-methyl 2-pyrolidene) is added with the mixture, and the slurry was made. Then, the slurry is applied on the $1 \times 1$ $cm^2$ area of nickel foam which was then dried at 70℃ for overnight for removing the solvent from the foam. The electrochemical properties of the fabricated electrode were analyzed in three electrode system using 1 M KOH as electrolyte solution. The active material-coated foam, Hg/HgO and platinum wire were used as the working electrode, reference electrode and counter electrode, respectively. Using the Biologic SP-300 Modular Research grade potentiostat/galvanostat/FRA electrochemical workstation, the electrochemical analysis was done. By applying the discharge time calculated in the galvanostatic charge–discharge (GCD) analysis in the formula below, the specific capacitance was calculated [16, 17]:

$$C_s = (I\Delta t)/(m\Delta V) \quad (1)$$

where, $I$ is the applied current density, $\Delta t$ is discharge time, $m$ is the mass of active material, $\Delta V$ is the potential window.

## Results and discussion

The analysis of phase purity and crystallinity for $NiWO_4$, both with and without the surfactant CTAB, was conducted using powder XRD. In Fig. 1, the X-ray diffraction (XRD) patterns of the prepared samples are illustrated. The primary diffraction peaks at $2\theta = 23.9°$, 24.9°, 30.9°, 36.5° and 54.6° correspond to the (011), (110), (111), (002) and (202) planes of the hexagonal NiWO4 crystal, aligning well with the (JCPDS.No.15–0755). For the as-synthesized NiWO4 sample, the characteristic peaks can be indexed as monoclinic

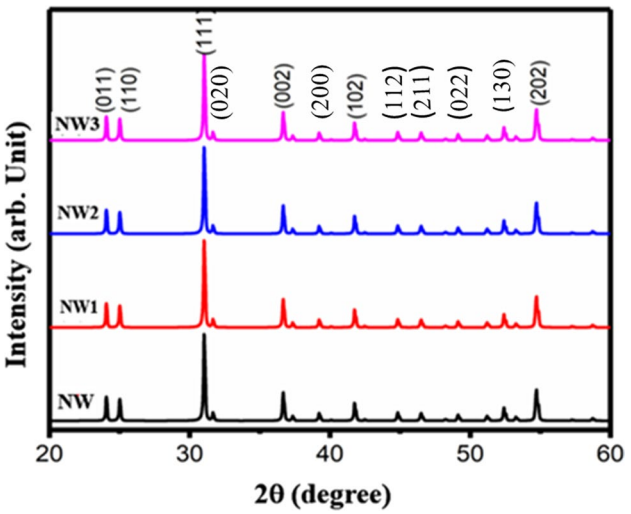


**Fig. 1** XRD patterns of prepared pure nickel tungstate and nickel tungstate at different ratio of CTAB

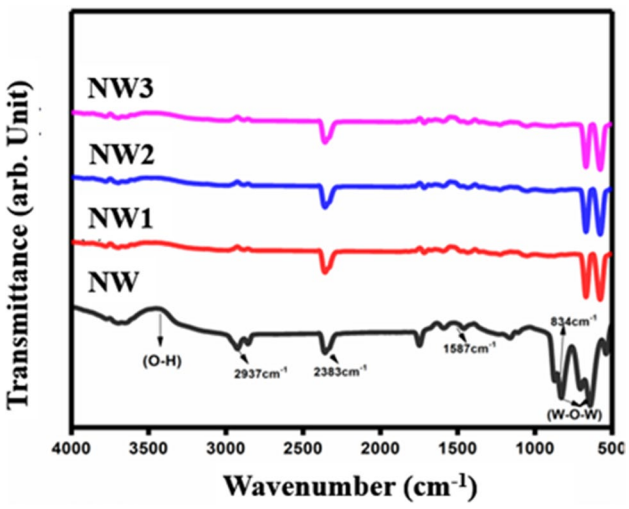


**Fig. 2** FT-IR spectrum of the nickel tungstate at different ratio of CTAB

$NiWO_4$. Importantly, there are no impurity peaks from reactants or intermediate phases, indicating the pure and highly crystalline nature of $NiWO_4$. Additionally, varying weight ratios of $NiWO_4$ with different CTAB ratios decrease the intensities of diffraction peaks proportionally. Crystallite size calculations using the Debye-Scherer Eq. (2) revealed that the crystallite sizes for the prepared $NiWO_4$ and different concentrations of CTAB (NW2, NW3) samples are 50.2, 48.3, 46.2 and 29.4 nm, respectively [18].

$$D = \frac{K\lambda}{\beta \mathrm{Cos}\theta} \tag{2}$$

where, $D$ is crystalline size, $K$ is Scherrer's constant ($K = 0.98$), $\lambda$ is the wavelength ($\lambda = 1.54$), $\beta$ is the full width at half maximum (FWHM).

The FTIR spectral analysis was carried out to identify the functional groups present in the samples (Fig. 2). The band observed at 834 $cm^{-1}$ could be assigned to the stretching of metal oxide (W–O) bond in terminal $WO_2$ group and 627 $cm^{-1}$ to O–W–O symmetric and asymmetric stretching vibrational modes respectively. Further, the band observed at 515 $cm^{-1}$ is due to the stretching vibrations of $NiO_6$ polyhedral in the crystal structure of $NiWO_4$. The absorption bands observed at 1587 $cm^{-1}$ and 2383 $cm^{-1}$ are typically attributed to the hydroxyl group of physically adsorbed water in the interlayers. The FT-IR spectra of NiWO4, prepared at various concentrations of CTAB, show no significant differences. The absence of absorption peaks from other organic functional groups in the FT-IR spectra confirms the purity of the sample [19].

The impact of a surfactant on the morphology of the prepared samples was investigated through SEM, as depicted in Fig. 3. The presence of surfactants notably influences the structural variations observed in the prepared samples. A clear distinction is apparent: particles synthesized without a surfactant exhibit unusually large sizes and significant agglomeration compared to those prepared in the presence of the surfactant (nanospheres).

As shown in Fig. 3a–b, pure $NiWO_4$ exhibits an irregular morphology with fine particles. For the closer inspection, images were analysed at a higher magnification and lower magnification from which the size was calculated. However, in the case of pure $NiWO_4$, it is difficult to calculate the exact particle size due to high degree of agglomeration. On the other hand, from Fig. 3c–h which is CTAB-assisted $NiWO_4$, a spherical morphology with a controlled size and low agglomeration rate was observed, attributed to the influence of CTAB. The addition of the surfactant (CTAB) efficiently decreased particle agglomeration and promoted a more even distribution. This is primarily associated with the formation process of nickel tungstate crystal nuclei. In the absence of a surfactant, the reaction between sodium tungstate and nickel nitrate initially generates crystal nuclei, with nickel tungstate nuclei growing as the reaction progresses. In the presence of the surfactant CTAB, nickel ions and CTAB form a complex through interactions between CTAB ions in the early stages. Subsequently, nickel tungstate grows along a specific direction, controlled by the surfactant CTAB. This has shown a significant effect on the particle nature, nucleation and the formation of $NiWO_4$ [13].

The electrochemical performance of the $NiWO_4$ with different concentrations of CTAB were analyzed using cyclic voltammetry, galvanostatic charge discharge and electrochemical impedance spectroscopy. Here, Fig. 4a represents the comparative CV response of prepared samples at a scan

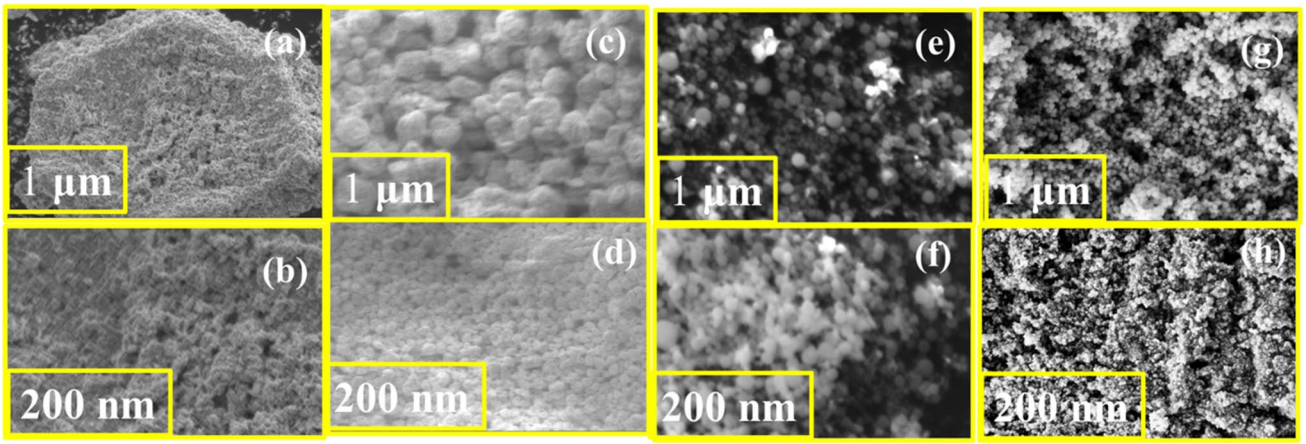


**Fig. 3** SEM images of **a**–**b** NW1, **c**–**d** NW1, **f**–**g** NW2, and **d** NW3

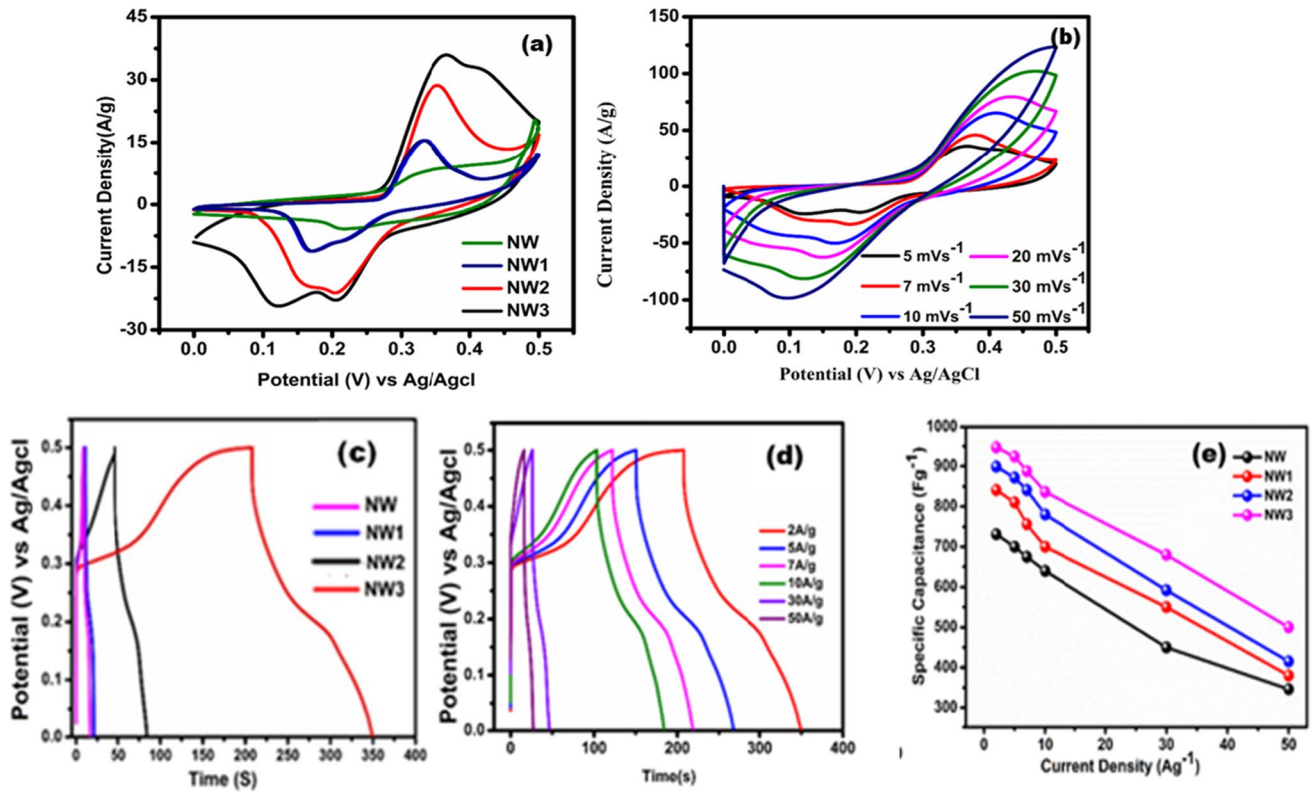


**Fig. 4** **a** Comparative CV curves of prepared samples at a scan rate of 5 mV/s, **b** CV curves of NW3 at various scan rates, **c** comparative GCD curves of prepared samples at a current density of 2 A/g, **d** GCD curves of NW3 at various current density, **e** specific capacitance graph of synthesized materials

rate of 5 mV/s. The obtained CV curve of $NiWO_4$, at all concentrations of CTAB, portrays the characteristic pattern of the redox material which were different from the ideal rectangular curve of EDLC, exhibiting its dominant pseudocapacitive properties. The well-resolved pair of faradic peaks may be ascribed to the reversible redox reaction of $Ni^{2+}$ and $Ni^{3+}$. In comparison of the area under the obtained CV spectrum, NW3 has the larger integral area which suggests its better specific capacitance with NW, NW1 and NW2. Further to study the rate capability, CV analysis of NW3 at different scan rates from 5 to 50 mV/s was performed and is displayed in Fig. 4b. Although, with a tenfold increase of scan rate, the CV curve almost retains its shape portraying the good reversible reaction of NW3. As the scan rate

increases, the intensity of redox peaks decreases due to sluggish faradic process, which in turn effectively reduces the specific capacitance. In addition, due to concise time at higher scan rate, a sufficient ionic diffusion cannot be achieved; rather, outer surface has been extensively utilized.

The two reduction peaks observed in cyclic voltammogram of $NiWO_4$ prepared with CTAB denote a cascade of redox activities of Ni and W species present in the solution matrix at the electrode surface, or it could mean different oxidation states of the nickel species in $NiWO_4$. Multiple reduction peaks can enhance specific capacitance by the following ways: (i) The presence of two reduction peaks may be ascribed to involvement of nickel and tungstate active sites on the electrode surface. This can lead to an increase in the effective surface area available for electrochemical reactions, thereby enhancing the overall capacitance; (ii) the observed different reduction peaks often correspond to distinct redox processes of nickel and tungstate at different potentials. This diversity in redox reactions can contribute to a broader range of charge storage mechanisms, resulting in a higher specific capacitance. (iii) Multiple reduction peaks can indicate a more complex electrochemical behavior, potentially involving intermediate species. This complexity might lead to improved charge transfer kinetics and enhanced overall electrochemical performance.

Galvanostatic charge discharge analysis was conducted for the sake of evaluating the electrochemical property or behavior of the as-synthesized samples, within the potential window of 0 to 0.5 V. Here in Fig. 4c, the comparative GCD curves of prepared samples at a current density of 2 A/g were displayed. The derived comparison with the prepared sample NW3 contains larger plateau region, and it projected that NW3 possess highly efficient redox performance than the other active materials. Here in Fig. 4d, the GCD curves of NW3 at various current density 2–50 A/g were portrayed and demonstrates their current response. From the GCD plot-specific capacitance of the synthesized sample at a current density of 2 A/g is calculated as shown in Fig. 4e. Here, the integrated area as well as the discharge time in both the CV and GCD of NW3 are greater when comparing with the other samples, and it displays its high electrochemical ability. However, the active mass of the active material is approximately 0.05 g in the Ni foam electrodes. The NW, NW1, NW2 and NW3 samples exhibited a specific capacitance of 718, 848, 906 and 958 F/g at a current density of 2 A/g respectively. The efficient performance of the sample NW3 might be due to which makes high active area for the interaction of electrolyte. Generally, the specific capacitance of the materials decreases with increase in current density of the four samples which may be ascribed to low interaction time of electrolyte with the electrode material. The sample NW3 delivers the highest capacitance among all samples due to its unique morphology which facilitated high active sites compared to other samples.

Nyquist plot of prepared sample is shown in Fig. 5a, and displays the linear line and a semicircle in low- and high-frequency range, respectively. It is seen from the plot that the lower diameter of semicircle for the NW3 compared to other samples represents its lower transfer resistance. The EIS curves at a high-frequency region have a intersect with $x$-axis at 0.2 Ω, revealing a representing its low-solution resistance and charge transfer resistance due to rapid transfer of electrons across the matrix and better contact of active material with electrolyte. Besides specific capacitance, their cycling stability is considered as one of the crucial properties of electrode material. The

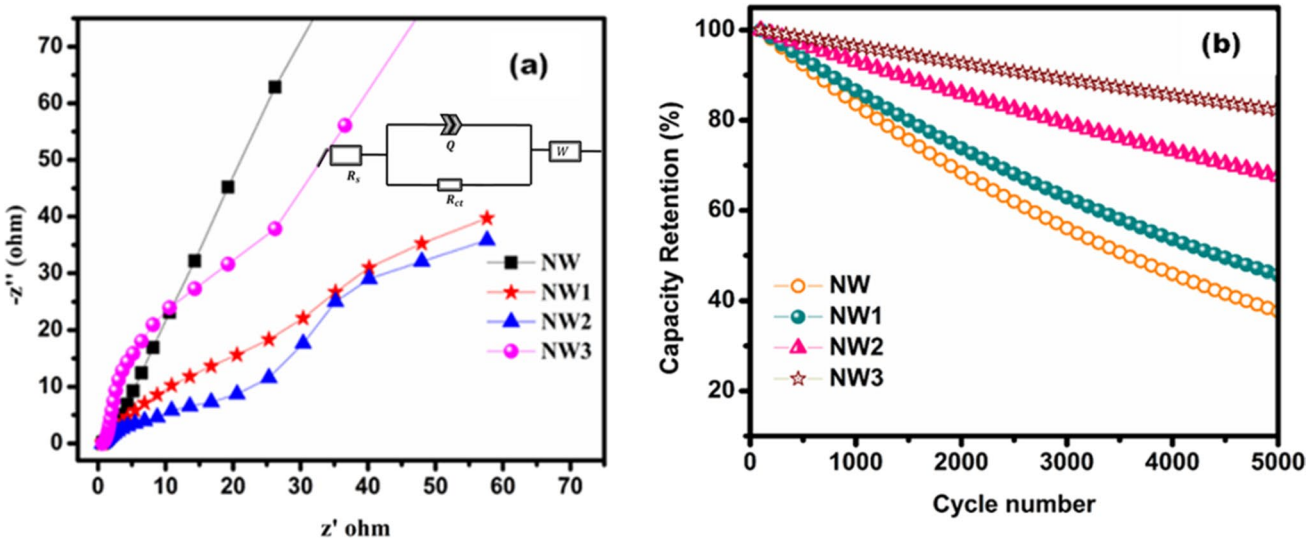


**Fig. 5** **a** Nyquist plots of prepared materials with a fitted equivalent circuit, **b** cyclic stability at a current density of 10A/g

charge transfer resistance ($R_{CT}$) values of the electrode materials NW, NW1, NW2 and NW3 calculated from the fitted circuit were1.9 Ω, 1.6 Ω, 0.98 Ω and 0.87 Ω. Among the electrode materials, NW3 has the least charge transfer resistance when compared to other materials resembling the better electrical conductivity and electrochemical property.

Capacitance retention of all the prepared samples after the cycling of 5000 cycles were shown in Fig. 5b. The better cycling ability of NW3 can be ascribed to good reversibility of faradaic reaction among its hybrid composites and also it with electrolyte. Hence, based on the electrochemical findings, it is evident that the optimal concentration of CTAB effectively alters the particle nature, thereby improving the mean free path and consequently enhancing the electrochemical performance of $NiWO_4$. The optimized morphology of NiWO4 prepared with CTAB provided easy electron transfer, short ion diffusion pathways and increased penetration of the ions into the electrode materials which was comparatively lower in agglomerated NiWO4 prepared without CTAB, which causes a drastic decrease in its cyclic stability.

## Conclusion

Concisely, $NiWO_4$ is synthesized by a facile hydrothermal technique method. Through various concentrations of CTAB added to $NiWO_4$, four different samples were prepared. Among the samples, NW3 delivered a better performance due to its spherical morphology compared to the other samples. The sample prepared with 0.03 M of CTAB delivers a higher specific capacity of 958 F/g at a scan rate of 2 A/g. It also delivered comparatively stable performance of 90% over 5000 cycles. Therefore, from the observed results, it is concluded that the concentration of CTAB played a key role in altering the morphology and size of particles and turns to play a vital role in the electrochemical performance of $NiWO_4$ for energy storage devices.

**Author contributions** K. Murugavel: Methodology, Investigation, Writing-Original Draft, Data curation. K.R. Hariprasath: Writing-Original Draft, Visualization. M. Priyadharshini: Software, Resources, Writing-review. P. Balaji: Methodology, Data curation. T. Pazhanivel: Validation, software, Investigation and N. Kannadasan: Supervision, Resources, Writing-review & editing. All authors read and approved the final manuscript.

**Data availability** Data will be made available on request.

## Declarations

**Ethics approval** Not applicable.

**Competing interests** The authors declare no competing interests.

## References


1. Conway BE (1999) Electrochemical supercapacitors scientific fundamentals and technological applications. Adv Lithium-Ion Batter. 481–505. https://doi.org/10.1007/0-306-47508-1_17
2. Zhang LL, Zhao XS (2009) Carbon-based materials as supercapacitor electrodes. Chem Soc Rev 38:2520–2531. https://doi.org/10.1039/b813846j
3. Yu A, Davies A, Chen Z (2012) Electrochemical supercapacitors. Electrochem Technol Energy Storage Convers 1:317–382. https://doi.org/10.1002/9783527639496.ch8
4. Priyadharshini M, Pazhanivel T, Bharathi G (2020) Carbon quantum dot incorporated nickel pyrophosphate as alternate cathode for supercapacitors. ChemistrySelect 5:2643–2652. https://doi.org/10.1002/slct.201904334
5. Priyadharshini M, Sandhiya M, Sathish M, Pazhanivel T, Mani G, Alothman AA, Alqahtani KN (2021) Surfactant-dependant self organisation of nickel pyrophosphate for electrochemical supercapacitors. J Mater Sci Mater Electron. https://doi.org/10.1007/s10854-021-07261-y
6. Zhu Y, Ji X, Pan C, Sun Q, Song W, Fang L, Chen Q, Banks CE (2013) A carbon quantum dot decorated RuO 2 network: outstanding supercapacitances under ultrafast charge and discharge. Energy Environ Sci 6:3665–3675. https://doi.org/10.1039/c3ee41776j
7. Matheswaran P, Karuppiah P, Chen SM, Thangavelu P, Ganapathi B (2018) Fabrication of g-C3N4 Nanomesh-anchored amorphous NiCoP2O7: tuned cycling life and the dynamic behavior of a hybrid capacitor. ACS Omega 3:18694–18704. https://doi.org/10.1021/acsomega.8b02635
8. Mohammadi Zardkhoshoui A, Ameri B, Saeed Hosseiny Davarani S (2022) Fabrication of hollow MnFe2O4 nanocubes assembled by CoS2 nanosheets for hybrid supercapacitors. Chem Eng J 435. https://doi.org/10.1016/j.cej.2022.135170
9. Vinoth S, Subramani K, Ong WJ, Sathish M, Pandikumar A (2021) CoS2 engulfed ultra-thin S-doped g-C3N4 and its enhanced electrochemical performance in hybrid asymmetric supercapacitor. J Colloid Interface Sci 584:204–215. https://doi.org/10.1016/j.jcis.2020.09.071
10. Rajeshkhanna G, Ranga Rao G (2018) Micro and nano-architectures of Co3O4 on Ni foam for electro-oxidation of methanol. Int J Hydrogen Energy 43:4706–4715. https://doi.org/10.1016/j.ijhydene.2017.10.110
11. Wang F, Zhan X, Cheng Z, Wang Z, Wang Q, Xu K, Safdar M, He J (2015) Tungsten oxide@polypyrrole core-shell nanowire arrays as novel negative electrodes for asymmetric supercapacitors. Small 11:749–755. https://doi.org/10.1002/smll.201402340
12. Reddy AE, Anitha T, Muralee Gopi CVV, Srinivasa Rao S, Kim H-J (2018) NiMoO 4 @NiWO 4 honeycombs as a high performance electrode material for supercapacitor applications. Dalt Trans 47:9057–9063. https://doi.org/10.1039/C8DT01245H
13. Huang Y, Gao Y, Liu C, Cao Z, Wang Y, Li Z, Yan Y, Zhang M, Cao G (2019) Amorphous NiWO 4 nanospheres with high-conductivity and -capacitive performance for supercapacitors. J Phys Chem C 123:30067–30076. https://doi.org/10.1021/acs.jpcc.9b08448
14. Ikram M, Javed Y, Shad NA, Sajid MM, Irfan M, Munawar A, Hussain T, Imran M, Hussain D (2021) Facile hydrothermal synthesis of nickel tungstate (NiWO4) nanostructures with pronounced supercapacitor and electrochemical sensing activities. J Alloys Compd 878:160314. https://doi.org/10.1016/j.jallcom.2021.160314
15. Jha S, Mehta S, Chen Y, Renner P, Sankar SS, Parkinson D, Kundu S, Liang H (2020) NiWO4 nanoparticle decorated

lignin as electrodes for asymmetric flexible supercapacitors. J Mater Chem C 8:3418–3430. https://doi.org/10.1039/c9tc05811g

16. Han Y, Liu N, Wang N, He Z, Liu Q (2018) Assembly of Ni-Al layered double hydroxide and oxide graphene quantum dots for supercapacitors. J Mater Res 33:4215–4223. https://doi.org/10.1557/jmr.2018.424
17. Zhang L, Ou M, Yao H, Li Z, Qu D, Liu F, Wang J, Wang J, Li Z (2015) Enhanced supercapacitive performance of graphite-like C3N4 assembled with NiAl-layered double hydroxide. Electrochim Acta 186:292–301. https://doi.org/10.1016/j.electacta.2015.10.192
18. Ikram M, Javed Y, Shad NA, Sajid MM, Irfan M, Munawar A, Hussain T, Imran M, Hussain D (2021) Facile hydrothermal synthesis of nickel tungstate (NiWO4) nanostructures with pronounced supercapacitor and electrochemical sensing activities. J Alloys Compd 878. https://doi.org/10.1016/j.jallcom.2021.160314
19. Xu X, Pei L, Yang Y, Shen J, Ye M (2016) Facile synthesis of NiWO4/reduced graphene oxide nanocomposite with excellent capacitive performance for supercapacitors. J Alloys Compd 654:23–31. https://doi.org/10.1016/j.jallcom.2015.09.108